Influence of reaction time, temperature and heavy metal zinc

characteristics of cellulose- and wood-derived hydrochars

from hydrothermal carbonization

- 5 Xin Zhao a, Jin Huang b *, Zhaonan Li c, Yao Chen d, Michael Müller a
- 6 a Institute of Energy and Climate Research, Microstructure and Properties of Materials (IEK2),
- 7 Forschungszentrum Jülich GmbH, 52425, Jülich, Germany
- 8 b Research Institute of Forestry, Chinese Academy of Forestry, 100091, Beijing, China
- 9 °School of Optical and Electronic Information, Hua Zhong University of Science and Technology, 430074, Wuhan, China
- dSchool of Chemical Engineering and Technology, Collaborative Innovation Center of Chemical Science and Engineering (Tianjin), Tianjin University, 300072, Tianjin, China

1415

16

17

18

19

20

21

22

23

24

25

13

1

3

4

Abstract

Hydrothermal carbonization (HTC) is a promising technique to convert biomass into valuable solid fuels. In this work, cellulose and wood-derived hydrochars were synthesized under hydrothermal carbonization conditions with different temperatures (200-250 °C) and reaction times (6 h or 12 h). The content of fixed carbon in the cellulose-derived hydrochar is higher than that of wood-derived hydrochar. Moreover, cellulose is easier to be carbonized during HTC reaction than wood. O/C and H/C ratios of all hydrochars were similar to those of lignite and decreased with increasing reaction temperature. The composition of solids recovered after 12 h is similar at all temperatures, consisting primarily of sp² carbons (furanic and aromatic groups) and alkyl groups. When a large amount of metal is introduced, except for part of the

¹ first author (Xin Zhao and Jin Huang contribute equally)

^{*} corresponding author. E-mail address: huangj@caf.ac.cn.

zinc combined with the energetic group, the remaining part will condense on the surface of the sample as zinc ions.

Keywords: Cellulose, Wood, HTC, Hydrochars, Lignite-like fuel, Heavy metal

Statement of Novelty

There is limited knowledge studied the format of heavy metals in wood- and cellulose-derived hydrochar during the HTC process and the release behavior of heavy metals under high temperatures. The impact of the reaction time, temperature, and heavy metal on characteristics of productions are systematically investigated. At high temperature, properties of hydrochars are similar to lignite-like fuel substances. The heavy metal element zinc is chosen to introduce into samples to simulate the heavy metal accumulation in biomass.

1. Introduction

In broad terms, biomass can be defined as a complex that contains all livings, dead creatures, and their waste[1]. Biomass can be used as carbonaceous material, which is the feedback of fossil fuel resources such as coal, lignite, etc. Currently, biomass contributes to 10 - 14% of total energy consumption in the world [2]. Moreover, biomass-derived fuels have the potential to solve the global energy crisis and alleviate environmental pollution caused by the combustion of traditional fossil fuels [3]. Therefore, biomass has been considered one of the most promising materials to replace non-renewable energy.

Several ways for biomass conversion toward valuable fuels such as pyrolysis, the biological conversion process, and HTC (hydrothermal carbonization) have been developed [4]. However, pyrolysis is not suitable for high moisture biomass waste because it needs high temperatures [5, 6]. The biological conversion processes, including fermentation and anaerobic

digestion, are economical but at the expense of conversion time [5, 7]. The HTC process is carried out under mild conditions, avoiding the use of unsafe conditions such as high temperature and high pressure [8]. HTC process includes reactions such as hydrolysis, dehydration, decarboxylation, aromatization, and re-condensation [9]. And similar to pyrolysis, the HTC process, generated hydrochars characterized by high carbon, high energy, low hydrogen, and oxygen [1, 8]. The emission of gases such as nitrogen oxides and sulfur oxides in water as acids or salts can be avoided during the HTC process [10]. HTC process has a low poisonous impact on materials, uses facile instrumentation and techniques, and effectively produces high energy and economy [11, 12]. Therefore, it is a suitable process for using biomass, even with high moisture contents that come from agricultural residues, wood, and herbaceous energy crops. In this respect, HTC has become an essential option for converting biomass to energy resources [13, 14].

Many experiments have reported that the hydrochars obtained by HTC can simulate the different low-rank coals [15, 16, 25, 17–24]. The temperature [26], reaction time [27], and pH [28] have different effects on the characteristics of hydrochar obtained by the HTC process. Also, the source of raw materials is an important factor that influences hydrochar properties. Numerous studies have mentioned hydrothermal carbonization of a variety of feedstocks such as bamboo [29], manure [30], sewage sludge [31], and municipal solid waste [32].

Because of urbanization, industrialization, and growth in pollution [32], the number of heavy metals is increased in biomass. Chemical, sewage sludge is a mixture of various organic and inorganic compounds. Several other elements, including heavy metals, are present in a variable content which are converted into the gaseous compounds during gasification [33]. The problem of pollution in biomass hinders the process of biomass conversion, it is also

- 73 significant to study it.
- 74 This work aims to investigate the effect of residence time and temperatures on the
- characteristics of the hydrochars produced from cellulose and wood via the HTC process, and
- also study the influence of heavy metals on hydrochars. This research can provide insight into
- the carbonization of cellulosic biomass and real biomass.

2. Materials and methods

79 *2.1. Materials*

- 80 Pure α -cellulose was purchased from Alfa Aesar. A-quality wood pellets were delivered by the
- 81 Labee Group in Moerdijk. The pellets were chopped into pieces (<0.54 mm) using an IKA
- laboratory mill. Zn(NO₃)₂ from Alfa Aesar, Teflon-lined stainless-steel autoclave is taper seat
- disc, 24*12~MC205HA. The vertical oven is from Prüfer Gmbh.
- 84 *2.2. Experimental procedure*
- 85 10 g of sample, 3 wt.% and 10 wt.% Zn(NO₃)₂ from Alfa Aesar, were suspended into 1L
- Teflon-lined stainless-steel autoclave. 50 ml of deionized water was added into the reactor, and
- then with a N₂ stream (100 mL/min) for 20 min to expel air, heated in a vertical oven at 200 or
- 88 250 °C (at a rate of 10 °C/min)[34]. The autoclave was transferred to an ambient temperature
- 89 environment after 6 h or 12 h reaction time. The solid residue was washed with deionized water
- and filtered several times until the pH value was neutral, and then dried at a temperature of 100
- °C in an oven for 12 h overnight [34].
- 92 2.3. Characterization
- The content of inorganic elements was measured via AAS. TGA measurement was
- performed to determine combustion behavior. A magnetic suspension balance with an online

mass spectrometer was used to measure the weight loss under combustion conditions at the temperature ranging from room temperature to 800 °C in an air atmosphere (20% O₂/N₂) heating rate of 10 °C/min. SEM images were acquired on a Zeiss SUPRA 50VP instrument to investigate the physical morphology of hydrochars. The functional groups' information of the samples was investigated by FTIR (Nicolet 6700 FTIR) with a diamond ATR accessory and a resolution of 2 cm⁻¹ from 4000 to 500. In terms of XPS analysis (Specs spectrometer), the binding energy of C 1s and O 1s were 284.82 eV and 532.75 eV, respectively.

3. Results and discussion

3.1. Combustion behaviors analysis

The detail components in the wood and cellulose have been shown in Table 1. Weight loss and rate of weight loss measurements are illustrated in Fig. 1, and the percentages of weight loss during the HTC reaction are shown in Table 2.

Table 1. Properties of different raw materials

Sample	Ash (%)	Cellulose (%)	Lignin (%)
Wood	5.3%	38%	29%

Table 2: Weight loss during three stages and residues of samples

Samples	Stage 1(%)	Stage 2 (%)	Stage 3 (%)	Loss (%)	σ
C-200-6	3.4	78.0	8.5	10.1	35.4
C-250-6	3.3	39.9	41.5	15.3	18.7
C-250-12	2.6	38.6	41.7	17.1	18.5

W-200-6	3.9	65.3	30.1	0.7	29.2
W-250-6	2.6	30.3	54.7	12.4	22.8
W-250-12	2.1	34.4	60.5	3	28.0

110 C: Cellulose, W: Wood, σ : standard deviation of Stage 1, Stage 2 and Stage 3

The first stage of TG-DTG (ambient to 100 °C) is for the evaporation of moisture. Changes of TG-DTG are similar at the first stage, indicating a similar content of moisture in cellulose-and wood-derived. A plateau between 110 and 190 °C follows, where the heating of molecules occurs without breaking chemical bonds.

The second stage is the combustion phase (200 - 400 °C), including devolatilization and combustion of volatile matters (e.g., moisture and small organic molecules) and sample combustion [35]. Wood-derived hydrochar and cellulose-derived hydrochar obtained by HTC reaction at 200 °C lost most of the weight during the second stage. Wood- and cellulose-derived hydrochars obtained at 200 °C lost more weight. Moreover, at the same HTC condition, the weight loss of cellulose-derived hydrochars is higher than that of wood-derived hydrochar. It indicates these hydrochars obtained at 200 °C are mainly made of volatile matters, and the content of volatile matters in cellulose-derived hydrochar is higher than that of wood-derived hydrochar.

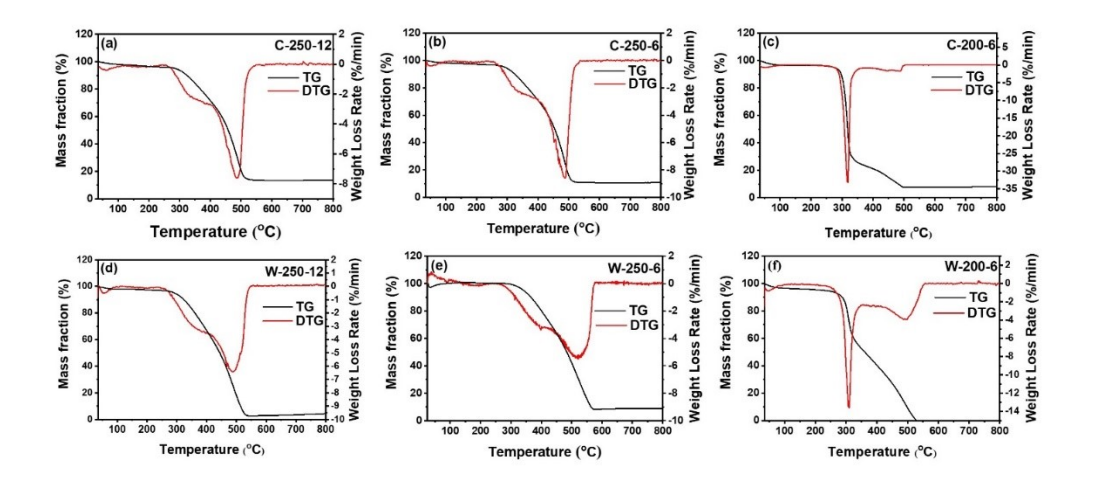


Fig. 1. TG and DTG images of different hydrochars: a) c-hydrochar 250 °C 12 h, b) c-hydrochar 250 °C 6 h, c) c-hydrochar 200 °C 6 h, d) w-hydrochar 250 °C 12 h, e) w-hydrochar 250 °C 6 h, f) c-hydrochar 200 °C 6 h.

The third stage, i.e., the burn-out stage (450 - 550 °C), is for the combustion of fixed carbon remaining after the preceding stages [36, 37]. Compared with the weight loss of hydrochars obtained at 250 °C in the third stage, the weight loss of hydrochars obtained at 200 °C is lower. That means more fixed carbon formed at 250 °C. At the same HTC reaction condition, the wood-derived hydrochar lost more weight than that of cellulose-derived hydrochar. It indicates the content of fixed carbon in wood-derived hydrochars is higher than that in cellulose-derived hydrochars. When HTC reaction temperature is 250 °C, the weight loss of the cellulose-derived hydrochars obtained at 6 h is similar to that of 12 h, meaning that fixed carbon does not change much with the increasing of time. While wood-derived hydrochar obtained in 12 h has significantly higher weight loss than that of 6 h. It means prolonging the reaction improves the content of fixed carbon for wood-derived hydrochar.

3.2. Structural properties of the hydrochars

Fig. 2 and Fig. 3 are the SEM images of cellulose-derived and wood-derived hydrochar. Because of the incomplete hydrothermal reaction, an irregular shape is shown in the SEM image of cellulose-derived (Fig. 2a) and wood-derived (Fig. 3a) hydrochar produced at 200 °C and 6 h reaction time. Hydrochars have a compact structure without any pores proves cellulose and wood dissolve incompletely due to the low temperature of the HTC reaction. The microspheres formed on the surface of hydrochars because sectional cellulose was solubilized and/or hydrolyzed. These nano/microspheres were also generated by the decomposition of amorphous cellulose [38].

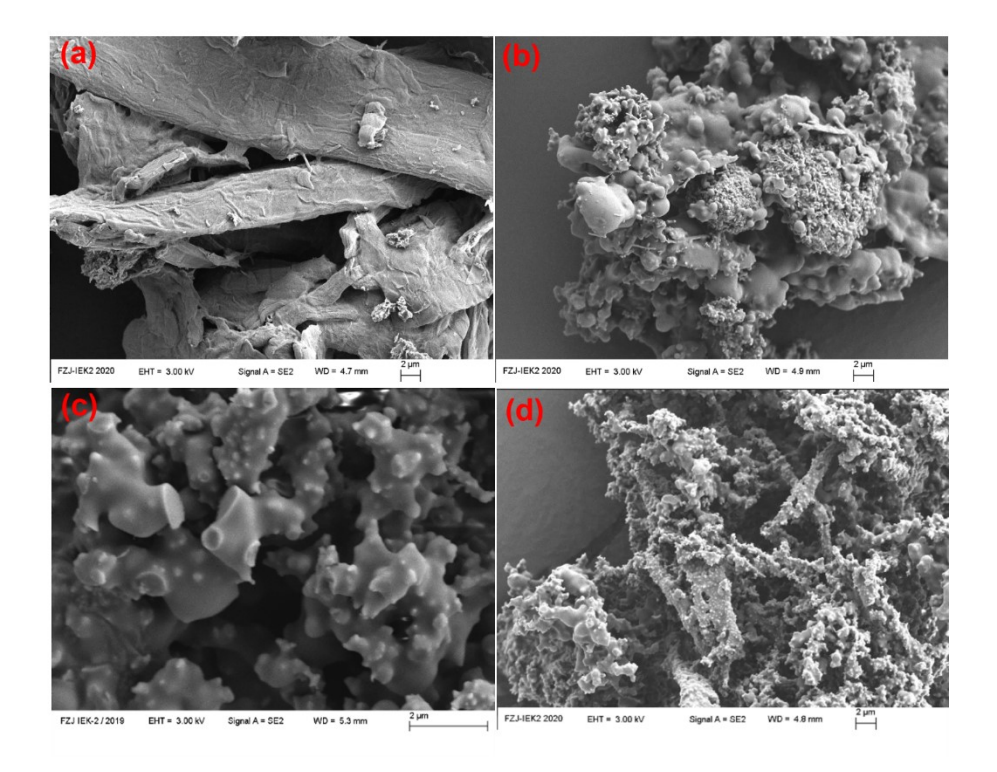


Fig. 2. SEM images of different c-hydrochars: a) 200 °C 6 h, b) 250 °C 6 h, c-d) 250 °C 12 h.

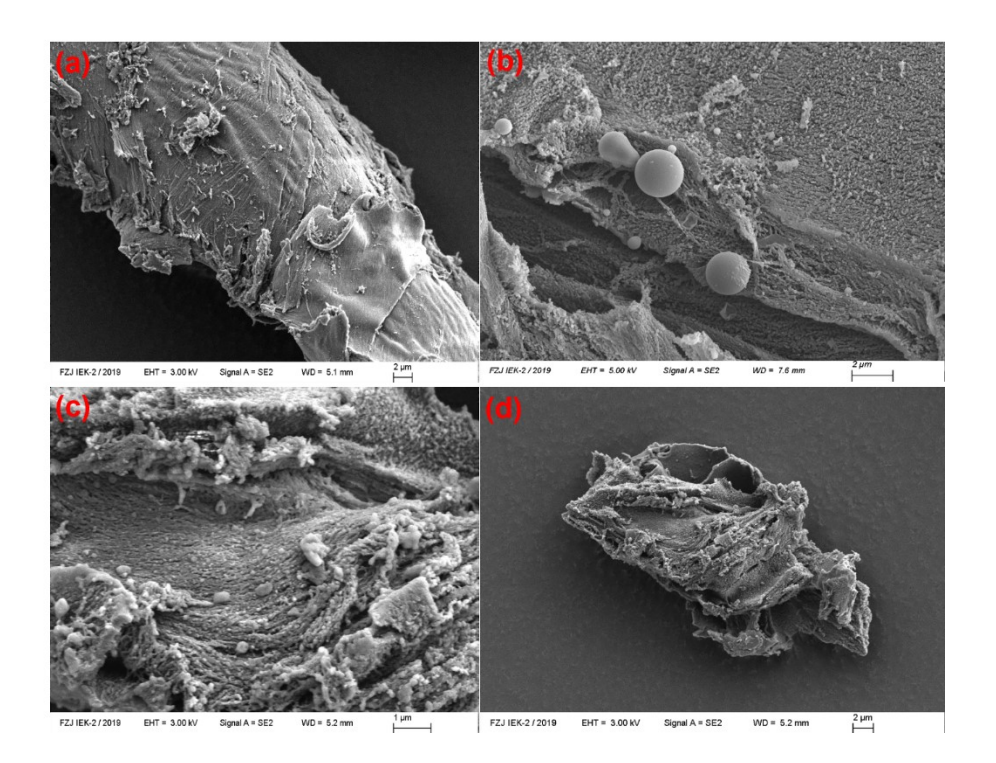


Fig. 3. SEM images of different w-hydrochars: a) 200 °C 6 h, b) 250 °C 6 h, c-d) 250 °C 12 h.

As shown in Fig. 2b and Fig. 3b, with 250 °C reaction temperature and 6 h reaction time, the surface of hydrochar became rougher as some pores and different sizes of small carbon microspheres were formed on the surface. One possible reason is that higher temperature facilitates the degree of solubility and/or hydrolysis of cellulose.

However, unlike cellulose-derived hydrochar, the microspheres formed on the surface of wood-derived hydrochar should be expected due to the conversion of hemicellulose, which is a fundamental component of wood [10]. The amount of sphere-like nano/microparticles of wood hydrochar is lower than that of cellulose-derived hydrochar under the same experimental conditions. It indicates that cellulose-derived hydrochar is much easier to be carbonized and/or hydrolyzed than wood-derived hydrochar.

It is illustrated in Fig. 2 (c-d) and Fig. 3 (c-d), after 12 h treatment, the dense structure shifted to a loose structure. Fig. 2c shows that parts of hydrochar are fused and adhered

between the microspheres at 250 °C after 12 h reaction time. The fragments and porosity of hydrochar increase due to gas emissions during devolatilization, and chemical bonds were broken. In Fig. 2d and 3d the degree of cellulose decomposition was more evident because the content of fixed carbon of cellulose-derived hydrochar is less than that of wood-derived hydrochar. Besides, the temperature can influence samples' structure by changing the properties of water, which easily permeates into the porous structure of hydrochars.

3.3 Chemical characterization

The elemental analysis of samples is shown in Table 3. Cellulose- and wood-derived hydrochars have a higher weight percentage of carbon and lower weight percentage of hydrogen and oxygen than their original substrates.

Table 3: The elemental analysis and the atomic ratio of raw biomass and hydrochars.

	Elemental analysis			atomic ratio		HCV ^b
						Kcal/kg
Samples	C (wt %)	H (wt %)	Oa (wt %)	H/C	O/C	
Cellulose	39.3	6.61	54.09	1.98	1.03	3170
C-200-6	41.60	6.03	52.37	1.74	0.94	3340
C-250-6	62.48	4.79	32.73	0.92	0.39	5072
C-250-12	63.30	4.50	32.20	0.85	0.38	5131
Wood	46.4	6.05	47.55	3.86	3.86	3752
W-200-6	57.80	5.92	36.28	1.23	0.47	4718
W-250-6	70.80	5.01	24.19	0.85	0.26	5789
W-250-12	71.90	4.93	23.17	0.83	0.24	5879

a: The amount of oxygen was calculated according to O (wt %) = 100-C (wt %) -H (wt %), b: calculated from Dulong formula

Higher HTC reaction temperature and longer reaction time can further increase the weight percentage of carbon and reduce hydrogen and oxygen weight. Normally, the H/C and O/C ratios were considered indicators for the degree of carbonization of hydrochars. The H/C atomic ratios are 1.74 (200 °C 6 h), 0.92 (250 °C 6 h), 0.85 (250 °C 12 h) for cellulose-derived hydrochar, and 1.23 (200 °C 6 h), 0.85 (250 °C 6 h) and 0.23 (250 °C 12 h) for wood-derived hydrochar. The O/C atomic ratios are 0.94 (200 °C 6 h), 0.39 (250 °C 6 h) and 0.38 (250 °C 12 h) for cellulose-derived hydrochar, and 0.47 (200 °C 6 h), 0.26 (250 °C 6 h), 0.24 (250 °C 12 h) for wood-derived hydrochar. The higher temperature and longer reaction can decrease the H/C and O/C ratios. The reduction of H/C means more condensed aromatic structures were produced due to aromatization as fundamental components of hydrochar. Aromatization also improves the stability of hydrochar in wood-derived hydrochar. The Decarboxylation process causes the reduction of the O/C by removing water from the raw materials without changing any chemical composition and producing CO₂, and CO [36, 39].

A Van Krevelen diagram is shown in Fig. 4. As a kind of low-rank coal, the atomic ratios of lignite are 0.8-1.3 (H/C) and 0.2-0.38 (O/C) [37], and the atomic ratio of synthetic hydrochars under 250 °C 6 h or 12 h is almost identical to that of lignite.

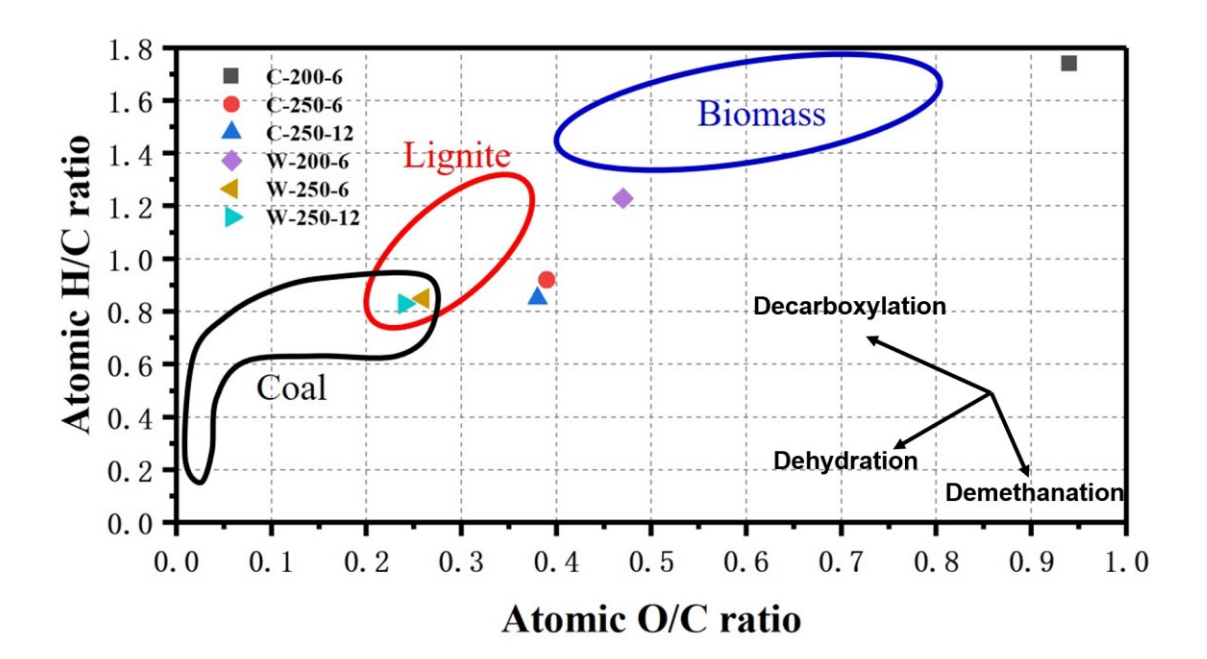


Fig. 4. Van Krevelen diagram of cellulose- and wood-derived hydrochar from hydrothermal treatment.

The results of the FTIR measurements were shown in Fig. 5. The band at 3000-3700 cm⁻¹ is assigned to the O-H stretching vibrations of hydroxyl or carboxyl groups [40]. Due to the dehydration reaction, the peak of O-H becomes weak with increasing HTC temperature. Furthermore, it was reported that O-containing functional groups could absorb heavy metal ions.

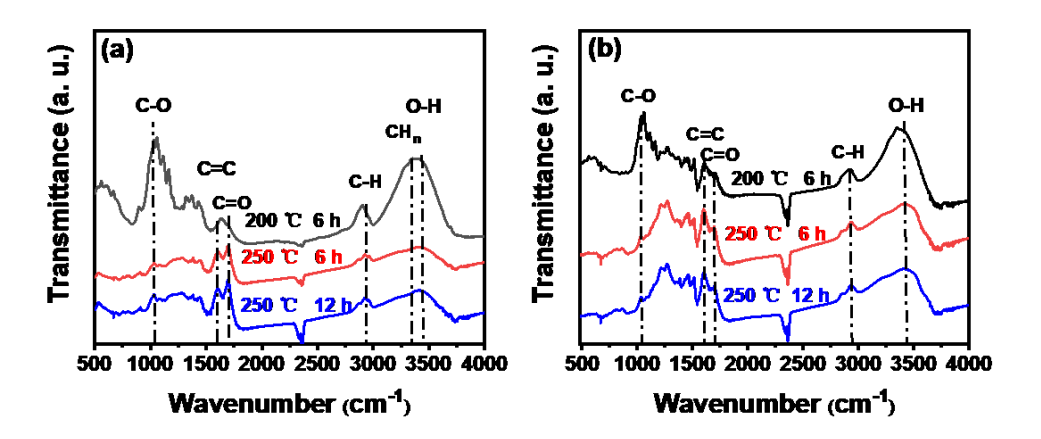


Fig. 5. FTIR spectra of hydrochars: a) HTC of celluose, b) HTC of wood.

The band at 2800-3000 cm⁻¹ is assigned to the stretching vibrations of aliphatic C-H,

indicating an aliphatic structure [41]. The unobvious curves ranging from 2800 to 3000 cm⁻¹ are attributed to the asymmetric stretching vibration of -CH₃ (2955 cm⁻¹) and -CH₂- (2922 cm⁻¹), symmetric vibration of -CH₃ (2871 cm⁻¹) and -CH₂- (2850 cm⁻¹), and stretching vibration of -CH (2900 cm⁻¹) [42]. The C-H vibration at around 2920 and 2850 cm⁻¹ is related to asymmetric and symmetric methylene stretching groups present in all the wood components [43]. The band at 1700 cm⁻¹ refers to C=O vibrations [39], while C=O belongs to the carboxyl group or carbonyl group, owing to the dehydration of hydroxyl [10]. The peak at 1620 cm⁻¹ is assigned to C=C vibrations of aromatic structures [44]. The peaks at 1120-1050 cm⁻¹ refer to the C=O bond.

The results show the peaks of C-O, C=O, and C-H in both cellulose-and wood-derived hydrochars decreased when reaction temperature increased. That is because more bonds (C-O, C=O, and C-H) breaks during hydrothermal treatment [10]. Gases such as CH₄, C₂H₆, and C₂H₄ are released when these bonds break and lead to the reduction of H/C and O/C ratio of hydrochar.

XPS analyzed the hydrocarbon and oxygen-containing functional groups of hydrochars, and the results are shown in Fig. 6. For cellulose-derived and wood-derived hydrochar, two main peaks of C (C1s) at around 285 eV and O (O1s) at about 530 eV are usually observed in the XPS spectroscope [45]. The peaks at 284.6 eV were attributed to CH_X and C-C/C=C, which belong to aliphatic/aromatic carbon groups. The peaks at 285.7 eV and 287.3 eV were contributed by hydroxyl groups (-COR) and carbonyl groups (C=O), respectively. The small peak observed at 289.2 eV can correspond to carboxylic groups, and esters (-COOR). It was also shown in the XPS results that the oxygen-containing functional groups such as hydroxyl groups, carbonyl groups, and esters existed on the surface of hydrochar.

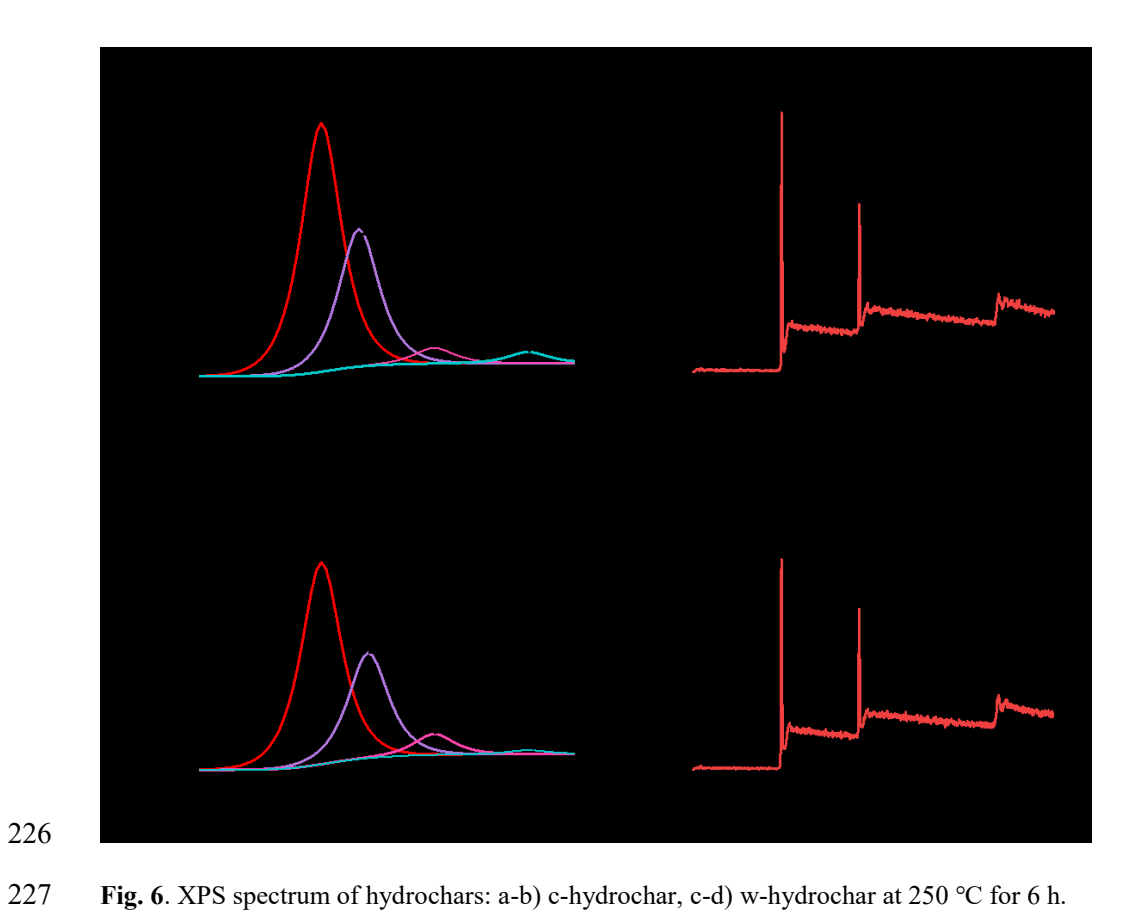


Fig. 6. XPS spectrum of hydrochars: a-b) c-hydrochar, c-d) w-hydrochar at 250 °C for 6 h.

228

229

230

231

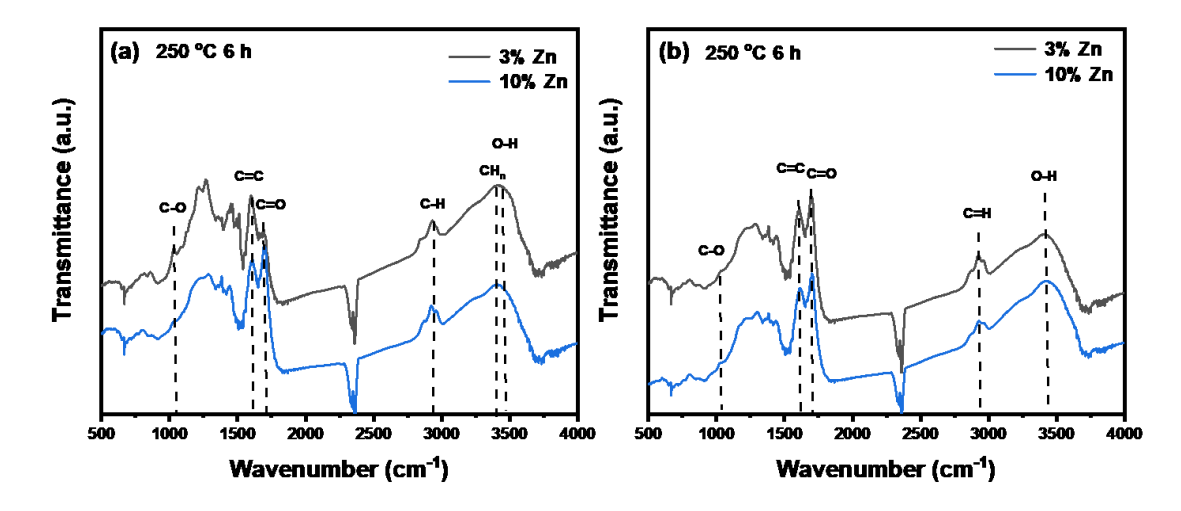


Fig. 7 FTIR spectra of hydrochars with heavy metals: a) HTC of cellulose with 3% and 10% zinc, b) HTC of wood with 3% and 10% zinc

Fig. 7 is the results of the FTIR measurements indicate that the types and positions of

functional groups of hydrochars after adding heavy metals are almost the same as those of hydrochars without heavy metals. Also, the SEM images of cellulose-derived and wood-derived hydrochar with heavy metals has been taken and it does not show the difference from the one without heavy metal.

The previous study found that the structure of benzoic acid which is adsorbed on (0001)-Zn decompose to benzene under 300 K [46] Therefore, it is supposed that the connection of Zn and carboxyl groups would promote decarboxylation reaction during the hydrothermal process. Moreover, Vohs et al. [46] reported that aromatic alcohols, benzyl alcohol, and phenol can form highly stable alkoxide species on the (0001)-Zn surface below 875 K. However, under high temperature, these organic functional groups are burned and zinc ions evaporate.

4. Conclusion

Cellulose and wood can be used to produce the carbon-rich and valuable hydrochars via hydrothermal carbonization. The results show that with the increment of temperature, the crystalline region is broken down stepwise, and the cellulose and wood are gradually converted into micro/nano carbon spheres. The hydrochars obtained at 200 °C are mainly composed of volatile matter. More prolonged reaction improves fixed carbon of wood-derived hydrochars form, but it has little impact on cellulose-derived hydrochars. Wood-derived hydrochar has more fixed carbon and condensed aromatic structures than cellulose-derived hydrochar. At 250 °C, their properties are similar to lignite-like fuel substances. Small amounts of heavy metals don't influence on the chemical and physical characteristics of hydrochar. More importantly, large amounts of zinc are introduced, zinc can be bonded to the surface of hydrochar by active groups which sheds light on the utilization of hyperaccumulator biomass from the remediation of heavy metal contaminated land.

Declarations

256

- Funding: This work has been performed in the framework of the HotVeGas Project supported by Bundesministerium für Wirtschaft und Technologie (FKZ 0327773).
- 259 Conflicts of interest/Competing interests: The authors declare that there is no conflict of interest Not applicable.
- Availability of data and material: All data generated or analyzed during this study are included in this published article.
- 263 Code availability: Not applicable.

Reference

- Tekin K, Karagöz S, Bektaş S (2014) A review of hydrothermal biomass processing. Renew Sustain Energy
 Rev 40:673–687. https://doi.org/https://doi.org/10.1016/j.rser.2014.07.216
- 267 2. Saxena RC, Adhikari DK, Goyal HB (2009) Biomass-based energy fuel through biochemical routes: A review. Renew Sustain Energy Rev 13:167–178. https://doi.org/https://doi.org/10.1016/j.rser.2007.07.011
- 269 3. Lehmann J (2007) A handful of carbon. Nature 447:143–144. https://doi.org/10.1038/447143a
- 270 4. Meyer S, Glaser B, Quicker P (2011) Technical, economical, and climate-related aspects of biochar
- production technologies: A literature review. Environ Sci Technol 45:9473–9483.
- 272 https://doi.org/10.1021/es201792c
- Wang T, Zhai Y, Zhu Y, et al (2018) A review of the hydrothermal carbonization of biomass waste for
- hydrochar formation: Process conditions, fundamentals, and physicochemical properties. Renew Sustain
- 275 Energy Rev 90:223–247. https://doi.org/https://doi.org/10.1016/j.rser.2018.03.071
- 276 6. Zhao P, Shen Y, Ge S, et al (2014) Clean solid biofuel production from high moisture content waste biomass
- 277 employing hydrothermal treatment. Appl Energy 131:345–367.

- 278 https://doi.org/https://doi.org/10.1016/j.apenergy.2014.06.038
- 7. Kwietniewska E, Tys J (2014) Process characteristics, inhibition factors and methane yields of anaerobic
- digestion process, with particular focus on microalgal biomass fermentation. Renew Sustain Energy Rev
- 281 34:491–500. https://doi.org/https://doi.org/10.1016/j.rser.2014.03.041
- 282 8. Liu F, Yu R, Ji X, Guo M (2018) Hydrothermal carbonization of holocellulose into hydrochar: Structural,
- 283 chemical characteristics, and combustion behavior. Bioresour Technol 263:508–516.
- 284 https://doi.org/https://doi.org/10.1016/j.biortech.2018.05.019
- Nizamuddin S, Baloch HA, Griffin GJ, et al (2017) An overview of effect of process parameters on
- hydrothermal carbonization of biomass. Renew Sustain Energy Rev 73:1289–1299.
- 287 https://doi.org/https://doi.org/10.1016/j.rser.2016.12.122
- 288 10. Kang S, Li X, Fan J, Chang J (2012) Characterization of hydrochars produced by hydrothermal
- 289 carbonization of lignin, cellulose, D-xylose, and wood meal. Ind Eng Chem Res 51:9023–9031.
- 290 https://doi.org/10.1021/ie300565d
- Wang Q, Li H, Chen L, Huang X (2001) Monodispersed hard carbon spherules with uniform nanopores.
- 292 Carbon N Y 39:2211–2214. https://doi.org/10.1016/S0008-6223(01)00040-9
- 293 12. Hu B, Wang K, Wu L, et al (2010) Engineering Carbon Materials from the Hydrothermal Carbonization
- 294 Process of Biomass. Adv Mater 22:813–828. https://doi.org/https://doi.org/10.1002/adma.200902812
- 295 13. Sharma HB, Sarmah AK, Dubey B (2020) Hydrothermal carbonization of renewable waste biomass for
- solid biofuel production: A discussion on process mechanism, the influence of process parameters,
- environmental performance and fuel properties of hydrochar. Renew. Sustain. Energy Rev. 123:109761.
- 298 https://doi.org/10.1016/j.rser.2020.109761
- 299 14. Ischia G, Fiori L (2020) Hydrothermal Carbonization of Organic Waste and Biomass: A Review on Process,
- Reactor, and Plant Modeling. Waste and Biomass Valorization. https://doi.org/10.1007/s12649-020-01255-3
- 301 15. Bergius F (1928) Beiträge zur Theorie der Kohleentstehung. Naturwissenschaften 16:1–10.
- 302 https://doi.org/10.1007/BF01504496
- 303 16. Berl E, Schmidt A (1928) Über das Verhalten der Cellulose bei der Druckerhitzung mit Wasser. Justus

304 Liebigs Ann Chem 461:192–220. https://doi.org/10.1002/jlac.19284610110 305 17. Berl E, Schmidt A, Koch H (1932) Über die entstehung der kohlen. Angew Chemie 45:517-519. 306 https://doi.org/10.1002/ange.19320453202 307 18. Berl E, Schmidt A (1932) Über die entstehung der kohlen. II. Die inkohlung von cellulose und lignin in 308 neutralem medium. Justus Liebigs Ann Chem 493:97-123. https://doi.org/10.1002/jlac.19324930106 309 19. Berl E, Schmidt A (1932) Über die Entstehung der Kohlen. III. Die Inkohlung von Harzen und Wachsen in 310 neutralem Medium. Justus Liebigs Ann Chem 493:124-135. https://doi.org/10.1002/jlac.19324930107 311 20. Dr. Hans Bode (1932) Die Inkohlung eine Druckverschwelung? 388–390. 10.1002/ange.19320452303 312 21. Cohen AD, Bailey AM (1997) Petrographic changes induced by artificial coalification of peat: comparison 313 of two planar facies (Rhizophora and Cladium) from the Everglades-mangrove complex of Florida and a 314 domed facies (Cyrilla) from the Okefenokee Swamp of Georgia. Int J Coal Geol 34:163-194. 315 https://doi.org/https://doi.org/10.1016/S0166-5162(97)00022-0 316 22. A Davis WS (1964) Role of cellulosic+ lignitic components of wood in artificial coalification. 43:215-224 317 23. Erdmann E (1924) Der genetische Zusammenhang von Braunkohle und Steinkohle auf Grund neuer 318 Versuche. Brennstoff-Chemie 5:177–186. https://doi.org/10.1016/j.fuel.2021.120600 319 24. Hwang I-H, Aoyama H, Matsuto T, et al (2012) Recovery of solid fuel from municipal solid waste by 320 hydrothermal treatment using subcritical water. Waste Manag 32:410–416. 321 https://doi.org/https://doi.org/10.1016/j.wasman.2011.10.006 322 25. Berge ND, Ro KS, Mao J, et al (2011) Hydrothermal carbonization of municipal waste streams. Environ Sci 323 Technol 45:5696-5703. https://doi.org/10.1021/es2004528 324 26. Li H, Wang S, Yuan X, et al (2018) The effects of temperature and color value on hydrochars' properties in 325 hydrothermal carbonization. Bioresour Technol 249:574-581. 326 https://doi.org/https://doi.org/10.1016/j.biortech.2017.10.046 327 27. Lu X, Pellechia PJ, Flora JR V, Berge ND (2013) Influence of reaction time and temperature on product

formation and characteristics associated with the hydrothermal carbonization of cellulose. Bioresour

- Technol 138:180–190. https://doi.org/https://doi.org/10.1016/j.biortech.2013.03.163
- Reza MT, Rottler E, Herklotz L, Wirth B (2015) Hydrothermal carbonization (HTC) of wheat straw:
- Influence of feedwater pH prepared by acetic acid and potassium hydroxide. Bioresour Technol 182:336–
- 332 344. https://doi.org/https://doi.org/10.1016/j.biortech.2015.02.024
- 333 29. Yan W, Perez S, Sheng K (2017) Upgrading fuel quality of moso bamboo via low temperature
- thermochemical treatments: Dry torrefaction and hydrothermal carbonization. Fuel 196:473–480.
- 335 https://doi.org/https://doi.org/10.1016/j.fuel.2017.02.015
- 336 30. Oliveira I, Blöhse D, Ramke H-G (2013) Hydrothermal carbonization of agricultural residues. Bioresour
- 337 Technol 142:138–146. https://doi.org/https://doi.org/10.1016/j.biortech.2013.04.125
- 338 31. Peng C, Zhai Y, Zhu Y, et al (2016) Production of char from sewage sludge employing hydrothermal
- carbonization: Char properties, combustion behavior and thermal characteristics. Fuel 176:110–118.
- 340 https://doi.org/https://doi.org/10.1016/j.fuel.2016.02.068
- 341 32. Jin Y, Lu L, Ma X, et al (2013) Effects of blending hydrothermally treated municipal solid waste with coal
- on co-combustion characteristics in a lab-scale fluidized bed reactor. Appl Energy 102:563–570.
- 343 https://doi.org/https://doi.org/10.1016/j.apenergy.2012.08.026
- 34. Gil-Lalaguna N, Sánchez JL, Murillo MB, et al (2014) Energetic assessment of air-steam gasification of
- sewage sludge and of the integration of sewage sludge pyrolysis and air-steam gasification of char. Energy
- 346 76:652–662. https://doi.org/https://doi.org/10.1016/j.energy.2014.08.061
- 347 34. Mai D, Wen R, Cao W, et al (2017) Effect of heavy metal (Zn) on redox property of hydrochar produced
- from lignin, cellulose, and d-Xylose. ACS Sustain Chem Eng 5:3499–3508.
- https://doi.org/10.1021/acssuschemeng.7b00204
- 35. Kalderis D, Kotti MS, Méndez A, Gascó G (2014) Characterization of hydrochars produced by
- hydrothermal carbonization of rice husk. Solid Earth 5:477. https://doi.org/10.5194/se-5-477-2014
- 352 36. Xiao L-P, Shi Z-J, Xu F, Sun R-C (2012) Hydrothermal carbonization of lignocellulosic biomass. Bioresour
- 353 Technol 118:619–623. https://doi.org/https://doi.org/10.1016/j.biortech.2012.05.060
- 354 37. He C, Giannis A, Wang J-Y (2013) Conversion of sewage sludge to clean solid fuel using hydrothermal

- carbonization: hydrochar fuel characteristics and combustion behavior. Appl Energy 111:257–266.
- 356 https://doi.org/10.1016/j.apenergy.2013.04.084
- 357 38. Gao Y, Wang X-H, Yang H-P, Chen H-P (2012) Characterization of products from hydrothermal treatments
- 358 of cellulose. Energy 42:457–465. https://doi.org/10.1016/j.energy.2012.03.023
- 359 39. Liu F, Guo M (2015) Comparison of the characteristics of hydrothermal carbons derived from holocellulose
- and crude biomass. J Mater Sci 50:1624–1631. https://doi.org/10.1007/s10853-014-8723-0
- 361 40. Sevilla M, Maciá-Agulló JA, Fuertes AB (2011) Hydrothermal carbonization of biomass as a route for the
- sequestration of CO₂: Chemical and structural properties of the carbonized products. Biomass and Bioenergy
- 363 35:3152–3159. https://doi.org/10.1016/j.biombioe.2011.04.032
- 364 41. Sevilla M, Fuertes AB (2009) The production of carbon materials by hydrothermal carbonization of
- 365 cellulose. Carbon N Y 47:2281–2289. https://doi.org/10.1016/j.carbon.2009.04.026
- 366 42. Ibarra J V, Miranda JL (1996) Detection of weathering in stockpiled coals by Fourier transform infrared
- 367 spectroscopy. Vib Spectrosc 10:311–318. https://doi.org/10.1016/0924-2031(95)00060-7
- 368 43. Poletto M, Zattera AJ, Santana RMC (2012) Structural differences between wood species: evidence from
- chemical composition, FTIR spectroscopy, and thermogravimetric analysis. J Appl Polym Sci 126:E337–
- 370 E344. https://doi.org/10.1002/app.36991
- 371 44. Sun X, Li Y (2004) Colloidal carbon spheres and their core/shell structures with noble-metal nanoparticles.
- 372 Angew Chemie 116:607–611. https://doi.org/10.1002/ange.200352386
- 373 45. Manyà JJ (2012) Pyrolysis for biochar purposes: a review to establish current knowledge gaps and research
- 374 needs. Environ Sci Technol 46:7939–7954. https://doi.org/10.1021/es301029g
- 375 46. Xu S, Adhikari D, Huang R, et al (2016) Biochar-facilitated microbial reduction of hematite. Environ Sci
- 376 Technol 50:2389–2395. https://doi.org/10.1021/acs.est.5b05517